Lithium oxide: a quantum-corrected and classical Monte Carlo study

M. Yu. Lavrentiev, [ID] *[a] N. L. Allan [ID] [b] and C. Wragg [ID] [b]

Extensive Monte Carlo simulations of lithium oxide, Li_2O, an important material for fusion applications over a wide range of temperatures have been performed. In the low temperature range 1–500 K, quantum path-integral corrections to the enthalpy and unit cell size were determined. We show that classical Monte Carlo underestimates both these quantities and the difference between unit cell parameters with and without quantum corrections is large enough that such corrections should be included in any comparison between theory and experiment. Over the range 300–1000 K, the formation energies of Schottky and Frenkel defects are calculated and compared with those from direct free energy minimisation in the quasiharmonic approximation, which also includes quantum corrections; the Monte Carlo results highlight the onset of failure of the quasiharmonic approximation even at modest temperatures and suggest only a small variation of the defect enthalpies with temperature. Several possible diffusion mechanisms are identified. While an interstitialcy mechanism activates at around 900–1000 K, lithium vacancy migration dominates from 500 K. The estimated migration energy of the Li-vacancy jump (0.28 eV) agrees very well with the most recent NMR study. At temperatures above 1000 K, the superionic phase transition and subsequent melting are simulated and there is good agreement with available experimental data. Our simulations predict a rapid rise in the heat capacity and the thermal expansion coefficient which continues up to the melting point which leaves two interesting questions for future experimental studies: (i) whether above the superionic transition the heat capacity and the thermal expansion coefficient in antifluorite Li_2O rise up to the melting point, as in our simulations, or fall, as observed in several fluorites, and (ii) the subsequent change in the heat capacity during melting.

1. Introduction

Lithium oxide, Li_2O, is a prospective material for use in fusion power plants as a blanket breeding material that converts high energy neutrons into heat and breeds tritium for the fusion reaction.[1,2] Li_2O has the antifluorite structure (space group $Fm\bar{3}m$), with the conventional cubic unit cell consisting of four O and eight Li atoms (see Fig. 1) and a lattice parameter a which varies between 4.6 and 4.7 Å, depending on temperature. Li atoms form a simple cubic lattice, while O atoms are packed in a face-centred cubic lattice. There have been numerous experimental and theoretical studies of its properties, mostly at high temperatures over 1000 K. These studies have confirmed the existence of a superionic phase transition at a temperature T_c between 1200 and 1350 K. Oishi *et al.*[3] in a study of lithium self-diffusion found a transition temperature close to 1273 K, while inelastic neutron scattering data by Hull *et al.*[4] suggests $T_c \approx 1350$ K and neutron diffraction experiments by Farley *et al.*[5]
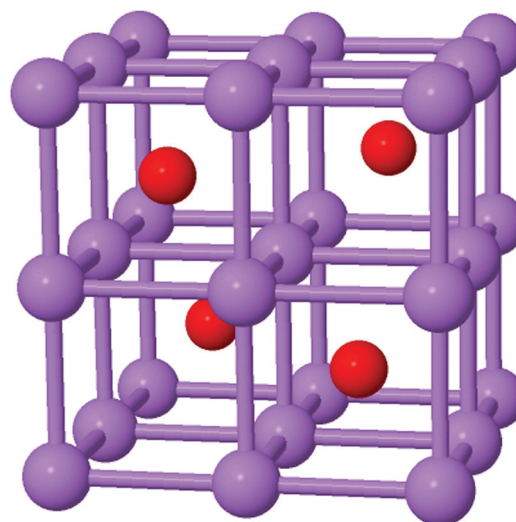

Fig. 1 Cubic unit cell of Li_2O. Red spheres represent oxygen atoms, violet spheres represent lithium atoms.

give $T_c \approx 1200$ K. This transition is related to disordering of the lithium lattice, while the oxygen lattice remains intact up to the

[a] United Kingdom Atomic Energy Authority, Culham Science Centre, Abingdon, Oxon, OX14 3DB, UK. E-mail: Mikhail.Lavrentiev@ukaea.uk

[b] School of Chemistry, University of Bristol, Bristol BS8 1TS, UK

melting point T_m (experimentally 1705 K [6] or 1711 K [7]). However, details of the disorder, the diffusion mechanism(s) below and above the transition temperature and the corresponding activation energies have been a matter of debate.[3,8–10]

The temperatures at which a lithium oxide breeding blanket is intended to work are between 680 and 1100 K,[11] a temperature range which has attracted less simulation-related research. In this work, we concentrate on low (<300 K) and intermediate temperature regions (300–1000 K). The former region presents an interesting opportunity for studying quantum effects due to the low mass of Li. Our aim here is to calculate quantum path-integral corrections to the Monte Carlo simulations of enthalpy, the unit cell size and volume, and compare with results of direct free energy minimization at the same temperatures using quasiharmonic lattice dynamics.[12–16] At intermediate temperatures, we investigate diffusion in the lithium subsystem below the superionic transition temperature. We also calculate the formation enthalpies of the most abundant defects: Schottky (Li and O vacancies) and Frenkel (Li vacancy and interstitial) and compare our results with experimental data and previous theoretical results. Finally, we briefly turn our attention to temperatures above 1000 K and compare our Monte Carlo results with experiment, and with previous molecular dynamics studies and contrast the temperature variation of the heat capacity of antifluorite Li_2O with that of fluorites.

2. Methods

Classical Monte Carlo simulations were performed on a system of 64 ($4 \times 4 \times 4$) unit cells with 768 atoms. Each simulation consisted of equilibration and accumulation stages; equilibration included 5×10^7 steps; in the accumulation stage 10^8 steps were performed. During one step of the Monte Carlo simulation a random decision is made to alter one of the variables of the calculation, which may either be an atomic position or one of the cell dimensions, *i.e.* all simulations are carried out within the *NPT* ensemble under ambient pressure and lattice vibrations are automatically included.[17] The magnitude of the change is also chosen at random, but within a specified amount and governed by the variables r_{max} and v_{max} respectively. The magnitude of these variables is adjusted automatically so that the acceptance/rejection ratio is 0.3. After each move/volume alteration the change in energy is calculated and a decision whether to accept or reject this is made according to the standard Metropolis scheme.[18]

A method that takes into account quantum corrections in Monte Carlo simulations is based on a discretization of the path-integral form of the density matrix[19] and is described in detail in ref. 20. It can be visualized as the replacement of each of the N atoms in a system by a "molecule" consisting of l atoms of the same species.[21] These atoms are joined together into a ring or polymer so that each of them interacts only with its two neighbours. This interaction is represented by a spring with coefficient

$$k = \frac{lmk_B^2T^2}{\hbar^2}, \qquad (1)$$

where m is the mass of the atom, k_B the Boltzmann constant, T the temperature and $\hbar$ the Planck constant. The equilibrium distance of the spring is zero, so that the lowest energy configuration of the molecule corresponds to all atoms being in one point. The classical interaction between the atoms belonging to different molecules is nonzero only between correspondingly numbered atoms, so that atom 1 of molecule 1 does not interact with atom 2 of molecule 2, *etc.* This interaction is scaled in accordance with the number of atoms in each "molecule":

$$V_{cl} = \frac{1}{l} \sum_{a=1}^{l} \sum_{i<j}^{N} v_{cl}(r_{ia} - r_{ja}), \qquad (2)$$

with indices i, j numbering atoms in the system and index a numbering atoms within a "molecule". This model can be relatively easily implemented in classical Monte Carlo programs and the main computational restriction that arises is related to the increase of overall number of atoms in simulation box from N to Nl. For path-integral Monte Carlo simulations performed in this study, each atom was replaced by a ring that could include $l = 2$, 4, or 8 atoms, so that the largest system studied included 6144 atoms. Larger systems need longer simulations in order to reach equilibrium, so for the cases of 4 and 8 atoms in a "molecule", the equilibration stage was extended to 10^8 steps.

Several interatomic interaction potentials have been developed for lithium oxide (see, *e.g.*, ref. 22–24). In the present study we used the potential developed by Fracchia *et al.*[25] from *ab initio* calculations and successfully applied to the study of the superionic transition,[25] as well as in a recent non-equilibrium molecular dynamics study of diffusion in Li_2O above 873 K.[10] Each short-range interaction is described by a Buckingham potential of the form

$$V(r) = A\exp\left(-\frac{r}{\rho}\right) - C/r^6, \qquad (3)$$

with parameters A, ρ, and C given in Table 1. Effective charges are +0.944 for Li and −1.888 for O (in units of $|q_e|$).

3. Low temperature properties and quantum effects

Over the temperature range 1 to 300 K, simulations were performed for l values of 1, 2, 4, and 8; for higher temperatures, only values of $l = 1$, 2, and 4 were used. The temperature dependence of the enthalpy and of the unit cell size for these values of l is shown in Fig. 2 (in Fig. 2a and everywhere in the text, quantities given per mole refer to a mole of Li_2O formula units). Similar behaviour is observed with increasing the size of

Table 1 Short-range Buckingham potential parameter set. A, ρ and C are defined in eqn (3). A cut-off of 8 Å was used

Interaction	A (eV)	ρ (Å)	C (eV Å^6)
Li–Li	0.0	1.0	0.0
Li–O	653.84	0.285723	0.0
O–O	0.0	1.0	76.651

This journal is © the Owner Societies 2019

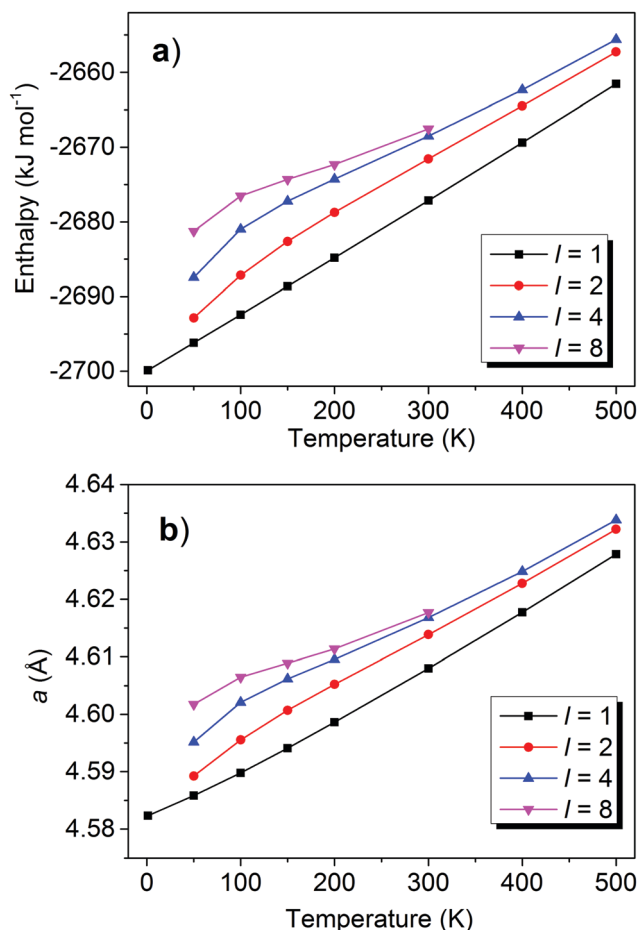*Phys. Chem. Chem. Phys.*, 2019, **21**, 14964–14972 | **14965**

Fig. 2 Enthalpy H (kJ mol^{-1}) (a) and lattice parameter a (Å) (b) of Li$_2$O as a function of temperature for values of the quantum path-integral Monte Carlo parameter l = 1, 2, 4, 8.

Fig. 3 Enthalpy H (kJ mol^{-1}) (a) and unit cell size a (Å) (b) of Li$_2$O in the limit of large quantum path-integral Monte Carlo parameter l vs. temperature. Blue lines are polynomial fits (see formula (5) for $H(T)$, (6) for $a(T)$). Free energy minimization results using the quasiharmonic lattice dynamics (QLD) and results obtained from classical Monte Carlo (l = 1) simulations are shown for comparison.

"molecules"; the magnitude of the enthalpy and unit cell parameter increase because of the effect of vibrations taken into account in Monte Carlo with path-integral corrections. This behaviour was found previously in studies of the free energy of a harmonic oscillator where exact solutions are available.[20,26] At lower temperatures, the parameter l must be large in order to reach convergence in the quantum-mechanical limit, as can be seen in Fig. 2 for the results at temperatures below 200 K.

In order to find the limit of enthalpy at large values of l, we approximated the enthalpy at each temperature between 100 K and 500 K as a function of l:

$$H(T,l) = H_\infty(T) + A(T)/l + B(T)/l^2, \qquad (4)$$

setting $B(T) = 0$ for 400 K and 500 K, since only three values of l were used at these temperatures. Next, values of the enthalpy in the limit of infinite l, $H_\infty(T)$ were fitted using the polynomial approximation (following ref. 27 and 28):

$$H_\infty(T) = H_0 + c_1 T^4 + c_2 T^6 + c T^8 \qquad (5)$$

The same procedure was performed for the unit cell parameter a, resulting in:

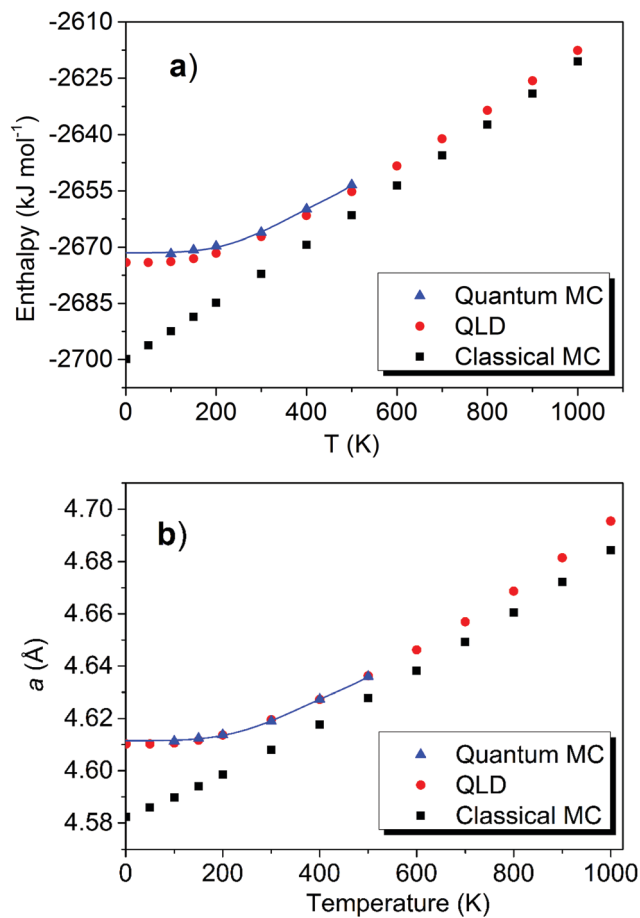$$a_\infty(T) = a_0 + d_1 T^4 + d_2 T^6 + d_3 T^8 \qquad (6)$$

In Fig. 3, we show the enthalpy and the unit cell parameter calculated using classical (l = 1) Monte Carlo and in the quantum limit, together with the respective polynomial fits. For comparison we have also calculated the unit cell size by direct free energy minimization in the quasiharmonic approximation[12–14] using the program GULP.[15,16] The convergence with the size of the Monkhorst–Pack grid[29] used to sum over phonon wave-vectors $\boldsymbol{k}$ in the Brillouin zone was checked. A 20 × 20 × 20 grid was found to provide sufficient accuracy – at temperatures 100 K, 500 K, and 1000 K increasing the grid to 32 × 32 × 32 k-points resulted in change of the enthalpy by less than 0.01 kJ mol^{-1} and the lattice parameter by less than 0.0003 Å. The agreement between path-integral Monte Carlo and GULP results is excellent, and at low temperatures both results substantially deviate from the classical Monte Carlo simulations. It is instructive here to compare our results with experiment and several other computational studies. While we are not aware of any experimental determination of the lattice parameter below 300 K, room temperature measurements are in the range 4.60 to 4.62 Å.[4,5,30] Hull et al.[4] have presented a fit of the lattice parameter based on measurements in the temperature

14966 | Phys. Chem. Chem. Phys., 2019, 21, 14964–14972

This journal is © the Owner Societies 2019

range 293–1603 K to terms in T and T^3. While this fit describes experimental data at and above 293 K very well, using an expansion with a leading linear term for lower temperatures[31–33] is questionable because of the functional form of the polynomial expansion for the lattice parameter valid at low temperatures (eqn (6)).[28] As Fig. 3(b) shows, the difference between the unit cell parameters calculated using quantum and classical methods can be as high as 0.03 Å close to 0 K, *i.e.* a rather substantial quantity which must be allowed for when comparing theory and experiment.

4. Defects and diffusion in solid state

The two most important types possible of defects in Li_2O are Frenkel and Schottky defects. The cation Frenkel defect is an interstitial Li^+ ion that has left a vacancy in the Li sublattice. The Schottky defect is the neutral combination of O and two Li vacancies.

In order to model a Frenkel defect, a single Li ion was removed from its position in the unit cell and placed in an interstitial position in the O sublattice, where it is surrounded by eight Li ions. The distance between the Li ion and the Li vacancy created by its removal was made as large as possible in order to minimize the Coulomb interaction between them. Classical Monte Carlo simulations were then performed at several temperatures between 1 and 300 K with a $4 \times 4 \times 4$ simulation box containing 768 atoms. To check the importance of quantum effects, path-integral simulations with values of the parameter $l = 2$ and $l = 4$ were also performed at 300 K. Similarly, the Schottky defect was modelled with two Li and one O vacancy situated as far away from each other as possible. For the Frenkel defect, annihilation of vacancy and interstitial was observed during the simulation at temperatures above 300 K for $l = 1$ and $l = 2$, so simulations were performed for $l = 4$, where both vacancy and interstitial remained in their positions during the whole run. Similarly, for the Schottky defect, clustering of the vacancies was observed at temperatures above 300 K for $l = 1$ and $l = 2$, in that the three vacancies migrated into nearest neighbour positions to each other. To avoid clustering, simulations at 500 K and 1000 K were also performed for the value $l = 4$.

Our results for defect formation enthalpies from the Monte Carlo calculations are compared with available experimental and theoretical data in Table 2. At the lowest temperature of 1 K, our calculated Frenkel and Schottky defect formation enthalpies are 2.28 eV and 4.77 eV, respectively. These values remain almost unchanged until 300 K, and indeed even over a temperature range of 1000 K change by only a few tenths of an eV. Increasing the parameter l at 300 K does not result in any substantial variation of the formation enthalpies: the Frenkel defect enthalpy decreases slightly to 2.19 eV, while the Schottky defect enthalpy remains unchanged. At 500 K, the formation enthalpies of both defects decreased slightly to 2.18 eV and 4.69 eV, respectively, with further decreases to 2.08 eV and 4.65 eV, respectively, at 1000 K. For comparison results obtained by direct free energy minimisation at each temperature using a $6 \times 6 \times 6$ cubic cell (2592 ions) are also shown in Table 2. Agreement with the Monte Carlo values at 1 K and 300 K is very good. The direct minimisation values fall off more rapidly with temperature than the Monte Carlo results, as can be seen from comparisons at 300 K and 500 K. This is associated with the onset of the failure of the quasiharmonic approximation in the free energy minimisation at the larger at interionic distances present even at relatively modest temperatures. This calls into question more generally the use of the quasiharmonic approximation for defect entropies and free energies at temperatures well below two-thirds of the melting temperature, at which the approximation is usually taken to break down in oxides such as Li_2O.[12] The small variation of the Monte Carlo defect enthalpies is in line with the general thermodynamic analysis of Taylor *et al.*[12]

Comparison with available experimental data, also listed in Table 2, shows that our results for high temperature formation enthalpy of Frenkel defect are in very good agreement with those obtained from the electric conductivity measurements of Chadwick *et al.* performed at temperatures up to 1300 K[34] and up to 1500 K.[35] Farley *et al.*[5] attempted to estimate the fraction of Li ions that leave their regular sites to occupy interstitial positions at high temperatures (up to 1603 K) from neutron diffraction data and report a lower formation energy value for the Frenkel pair of $\sim$2.1 eV which almost coincides with our value at 1000 K. Note however that the model-dependent estimate of the number of interstitials in ref. 5 assumes the

Table 2 Comparison of values of Frenkel and Schottky formation enthalpies obtained in this work with available experimental and calculated values for enthalpies or energies (*) (eV)

| | This work | | | | |
| | Temperature (K) | | | | |
Type of defect	1	300	500	1000	Literature values
Frenkel (experimental)	—	—	—	—	2.1*,[5] 2.53,[34] 2.6[35]
Frenkel (calculated, Monte Carlo)	2.28	2.30 ($l = 1$) 2.25 ($l = 2$) 2.19 ($l = 4$)	2.18 ($l = 4$)	2.08 ($l = 4$)	2.12,[34] 2.37,[35] 2.55*,[36] 1.98*,[37] 2.2*,[38] 1.7*–2.2* (ref. 32 five different potentials), 2.0*,[39] 1.93–2.33* (ref. 22 four different potentials)
Frenkel (calculated, free energy minimisation)	2.28	2.15	2.00	—	
Schottky (calculated)	4.77	4.74 ($l = 1$) 4.68 ($l = 2$) 4.74 ($l = 4$)	4.69 ($l = 4$)	4.65 ($l = 4$)	5.15,[34] 5.24,[35] 5.8*,[36] 4.73*[37]
Schottky (calculated, free energy minimisation)	4.82	4.61	4.38	—	

Li ion interstitial position is midway between two regular site cations. Our Monte Carlo simulations show that interstitial Li ions always lie in an octahedral hole, *e.g.*, the centre of a cube formed by eight cations, except when the ion moves from one cube to another. Our results agree with previous calculations confirming that Schottky defects are considerably higher in energy than Frenkel and thus the defect chemistry of Li_2O will be dominated by almost equal concentrations of lithium vacancies and lithium interstitials.

As mentioned above, at elevated temperatures Monte Carlo runs include jumps of Li ions, as well as Li-vacancy recombination. This makes it possible to investigate the nature of Li diffusion in Li_2O and to estimate the Li vacancy migration energy from the simulations. First, we studied the types of movements of Li interstitials in the lattice. Snapshots of 5000 configurations obtained during accumulation stage of Monte Carlo run in large (6144 atoms) simulation boxes with a single Frenkel defect were stored and the positions of the interstitial atom relative to the centre of mass of the simulation box calculated. At temperatures of 500 K and 700 K, the coordinates of this atom change very little and it remains near its initial position for the entire run. For example, the standard deviation of the interstitial Li position from that averaged at 700 K is only about 0.07–0.08 of the corresponding nearest neighbour Li–Li distance along each of the crystallographic axes. Calculation at the same temperature for the eight surrounding Li cations shows that they also remain near their crystallographic positions, with a slightly smaller standard deviation of 0.06–0.07 of the nearest neighbour Li–Li distance. At 900 K, a single jump of the interstitial atom into the position of a neighbouring cation was detected in the accumulation stage of the simulation (10^8 steps), with a corresponding jump of the displaced cation into another interstitial position (an interstitialcy mechanism), resulting in overall interstitial displacement by $r = (a/2, 0, -a/2)$ away from its initial position. Several such jumps occur at $T = 1000$ K. Thus, the interstitialcy mechanism of Li diffusion activates around 900–1000 K.

The majority of large (of the order of interatomic distance) changes of position of Li atoms were found to be Li-vacancy exchanges. The first such exchange was detected at a temperature as low as 500 K. All such migrations were between a vacancy and one of its six nearest neighbour Li atoms along the (100) direction. A part of the path of the vacancy in simulation box via such exchanges recorded at 900 K is shown in Fig. 4. Calculations of migration enthalpy usually employ only quasi-harmonic lattice dynamics or molecular dynamics methods.[40] Monte Carlo simulations have been rarely used (*e.g.*, the difference Monte Carlo study of Ar, Ag, and Cu by De Lorenzi *et al.*,[41] performed on a small system of 31 atoms in a 32-site simulation box). The current simulations that include Li-vacancy jumps at several temperatures provide an interesting opportunity to estimate the migration energy for vacancy-mediated Li diffusion in a Monte Carlo run. To do this, the logarithm of the number of jumps during the accumulation stage is plotted as a function of inverse temperature between 500 K and 1000 K (Fig. 5). The temperature dependence is indeed almost linear and from the gradient the migration energy is ∼0.28 eV. This value agrees well with the
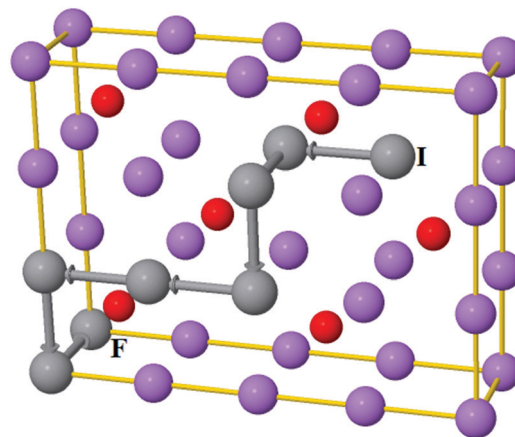

Fig. 4 Part of the path of a vacancy generated in a Monte Carlo run at temperature $T = 900$ K with a single Frenkel defect in the simulation box. Vacancy is represented by grey spheres. Initial and final positions of the vacancy are denoted I and F, respectively. Each vector shows single vacancy hop, accompanied by reverse hop of the Li atom.
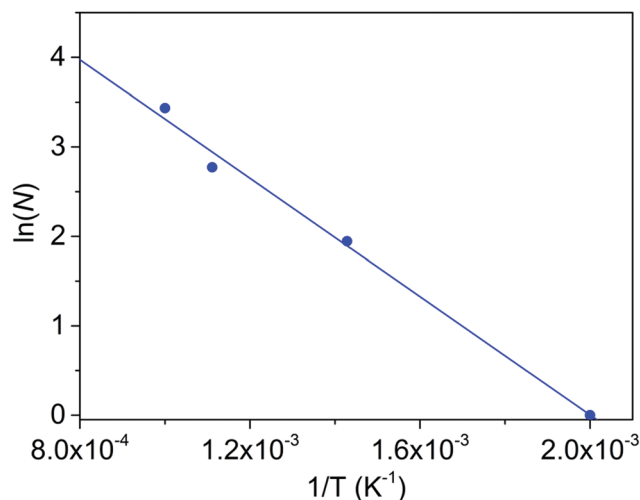

Fig. 5 Temperature dependence of the logarithm of the number N of Li cation jumps during the simulation. The straight line is a linear fit: $\ln(N) = 6.61968 - 3308.1765$ K/T.

majority of previous theoretical estimates of the vacancy migration energy: 0.21 eV,[34] 0.26 eV,[36] 0.34 eV,[38] 0.28–0.33 eV,[42] 0.28 eV.[10] Most of these theoretical calculations lie below the previously reported experimental vacancy migration enthalpies of 0.49 eV,[34] 0.5 eV[35] or ∼0.4 eV.[8] One possible reason for this discrepancy might be the association of the vacancies, either with O vacancies, or with positively charged impurity ions, such as Mg^{2+}. However, the most recent experimental NMR study reports a value of 0.31 eV,[43] in excellent agreement with calculation.

Large Li-ion hops far away from both vacancy and interstitial were observed only at the highest studied temperature, 1000 K. They include hops of a single atom into a neighbouring position along the (100) direction followed by it returning back or by the atom displaced by it hopping shortly thereafter to the initial lattice site. Such hops correspond to the emergence of the soft mode, discussed in ref. 25 at the edge of the Brillouin

14968 | *Phys. Chem. Chem. Phys.*, 2019, **21**, 14964–14972

This journal is © the Owner Societies 2019

zone in the [100] direction. Softening of this mode as well as of the [110] transverse acoustic mode at the zone boundary was found also in ref. 44. These modes involve movements of Li ions only in the [100] direction and indicate the approach of the superionic transition. Also, we saw a single event of a coordinated four Li ion jump in a closed square loop, similar to those found by Mulliner *et al.*[10] at 973 K. We did not investigate Li diffusion at temperatures above 1000 K, so we were unable to observe defect-free interstitial-related diffusion seen in ref. 10 in the superionic regime. However, we can see now that addition of a Frenkel defect allows rather accurate estimate of the vacancy-mediated migration energy in the temperature range 500–1000 K.

5. Melting and the superionic phase transition

Changes related to the superionic transition and melting were studied by calculating several properties of Li_2O. We have examined unit cell size and enthalpy as well as the heat capacity. Further, structural changes in the lattice were investigated by calculating the radial correlation functions $g(Li–Li)$ and $g(O–O)$, calculated from interatomic distances using snapshots of 5000 configurations obtained during the accumulation stage of Monte Carlo run (details of calculation are given in Ch. 6 of ref. 20). An example of radial correlation functions calculated at 1000 K (below both transitions) is given in Fig. 6.

An important point concerning high-temperature Monte Carlo simulations is the choice of initial configuration. If the run begins with the ideal crystal lattice, the absence of interfaces, due to the periodic boundary conditions, can result in over-heating phenomena that lead to an overestimation of the melting temperature. Simulations that start with a mixed initial configuration are a more reliable method of finding the melting point. At temperatures above 1000 K we used both approaches. In the first, simulation started from the solid configuration with atoms in their ideal positions. In the second, initially a simulation at very

high temperature $T = 2400$ K was performed that resulted in a final liquid configuration. Half of that configuration was taken, and the simulation box completed with ideal solid configuration, so that the starting configuration was half-solid and half-liquid.

First, we calculated the melting temperature of Li_2O. Until now, two studies with the current potential were performed that gave contradictory results. Fracchia *et al.*[25] estimated the melting point to lie between 1700 K and 1900 K. However, later work with the same potential[22] found a very high melting point of 2250 K, estimated from a sharp rise in the lattice parameter. In both studies, molecular dynamics simulations were performed, making the large disagreement between ref. 22 and 25 even more puzzling. Our results for the unit cell parameter calculated from the two different initial configurations are shown in Fig. 7a and they are strikingly different above 1500 K. The simulation with entirely solid initial configuration exhibits a jump of the unit cell parameter between 2100 K and 2200 K, close to the results reported in ref. 22. For the mixed solid–liquid configuration, the corresponding jump takes place between 1500 K and 1550 K, much closer to the experimental melting point of 1705 K[6] or 1711 K,[7] as well as to the results reported in ref. 25. Thus, an initial mixed configuration results in a more realistic value of the melting temperature, and so we used calculations with mixed configuration throughout the high-temperature simulations. Melting in the region 1500–1550 K from the initial mixed configuration is also confirmed by a jump in the enthalpy (Fig. 7b) and abrupt fall in the height of the maximum of the radial distribution functions, *i.e.* the first peak (Fig. 7c) both for Li–Li and O–O.

The superionic transition manifests itself in several ways. First, a broad maximum of the heat capacity that begins in our simulations at about 1100 K and continues until the melting of the crystal (Fig. 8), is observed. All of the available experimental data on heat capacities (Tanifuji *et al.*,[45] who also includes results from ref. 46–48) are restricted to temperatures below 1125 K, thus omitting the superionic transition range. The fit by Barin and Knacke[48] that extends up to 1843 K is shown in Fig. 8. The molecular dynamics study by Wilson *et al.*[49] found a superionic transition-related peak in the heat capacity at $\sim$1450 K with a subsequent decrease well below the melting point. In our simulations, however, the heat capacity rises all the way up to the melting point, where the heat capacity abruptly falls by about 30 J mol^{-1} K^{-1} (Fig. 8). Further experimental studies of the heat capacity up to and beyond the melting point are highly desirable. The entropy of the superionic transition in our study is similar to that found in ref. 49: integrating the excess of the heat capacity over the fit shown in Fig. 8, we obtained a transition entropy of about 6.45 J mol^{-1} K^{-1}, or $0.78R$, close to 5.8 J mol^{-1} K^{-1}.[49] Both these estimates are below the experimental values for superionic conductors with the fluorite (rather than antifluorite) structure such as $SrCl_2$, CaF_2, and PbF_2 that are in the range 15–16.5 J mol^{-1} K^{-1}.[50,51] A possible explanation of this difference is that in Li_2O, the transition to superionic state may be interrupted by the melting. Another manifestation of the superionic transition is the faster than linear increase of the thermal expansion coefficient starting
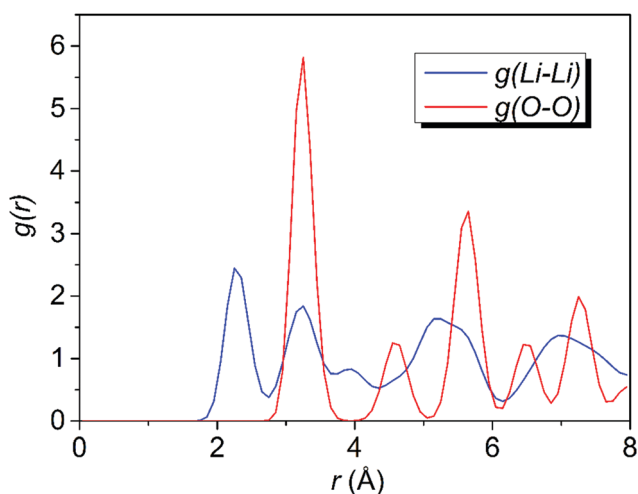

Fig. 6 Radial distribution functions $g(Li–Li)$ (blue) and $g(O–O)$ (red), calculated at $T = 1000$ K.

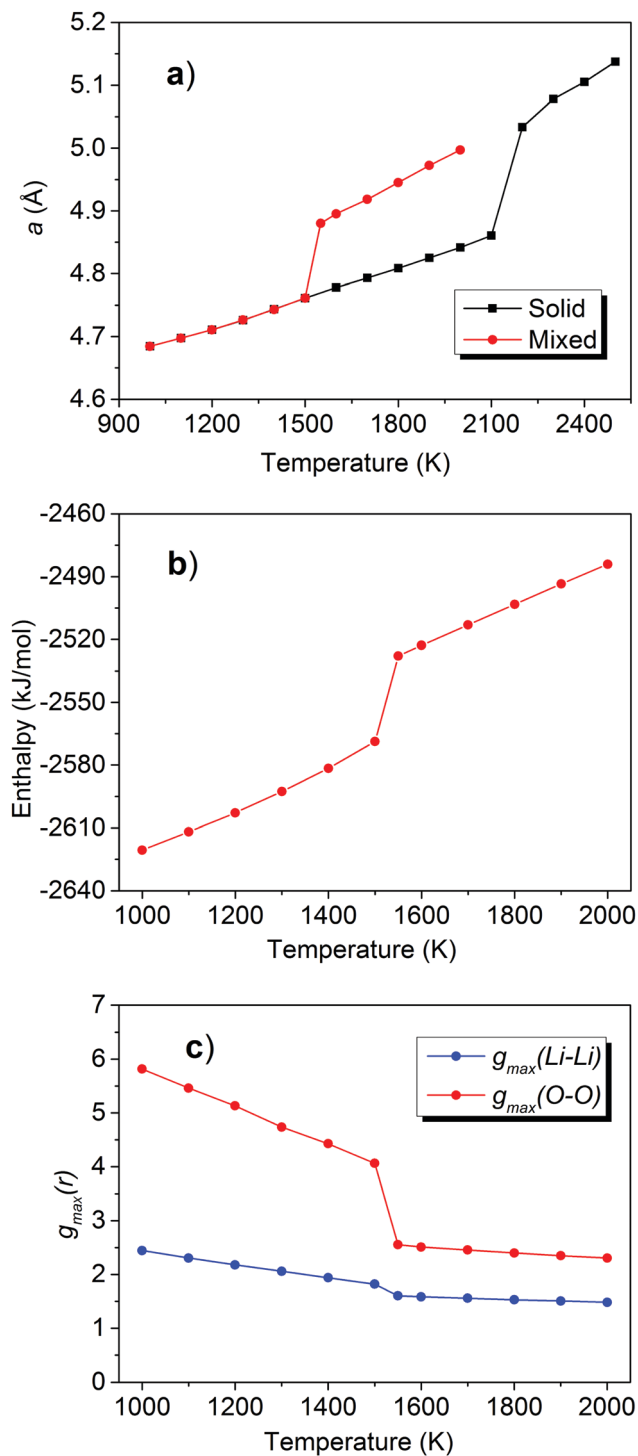This journal is © the Owner Societies 2019

Phys. Chem. Chem. Phys., 2019, **21**, 14964–14972 | 14969

Fig. 8 Heat capacity of Li$_2$O calculated starting from mixed (half-solid, half-liquid) system (red) compared with extrapolation from low temperature data (Barin and Knacke,[48] as reported in ref. 45).

expansion coefficient with temperature is observed.[52] Finally, rapid increase of the mobility of Li ions above 1200 K can be seen in the calculated mean square displacements. While the

Fig. 7 Unit cell size a (Å) $vs.$ temperature for simulations starting from solid (black) and mixed solid–liquid (red) systems (a); enthalpy H (kJ mol^{-1}) $vs.$ temperature for simulation starting from mixed (half-solid, half-liquid) system (b); maximum value of the radial distribution functions g(Li–Li) and g(O–O) $vs.$ the temperature of the simulation starting from the mixed (half-solid, half-liquid) system as described in the text (c).

Fig. 9 Thermal expansion coefficient of Li$_2$O (red line and points) $\alpha = (\mathrm{d}a/\mathrm{d}T)/a$ numerically calculated from the Monte Carlo results for the lattice parameter $a(T)$ (a), straight blue line is a linear fit of $\alpha(T)$ between 400 K and 900 K; mean square displacement of Li and O atoms during the accumulation stage of Monte Carlo run (b).

from about 1200 K (Fig. 9a). As with the heat capacity, the rise continues all the way up to the melting point, in contrast to fluorites where a clear maximum in the variation of the
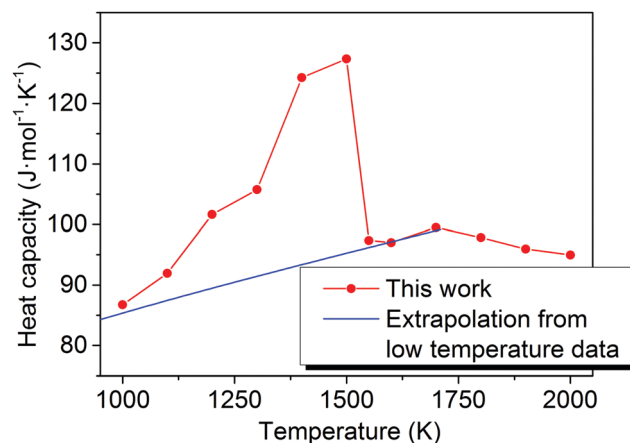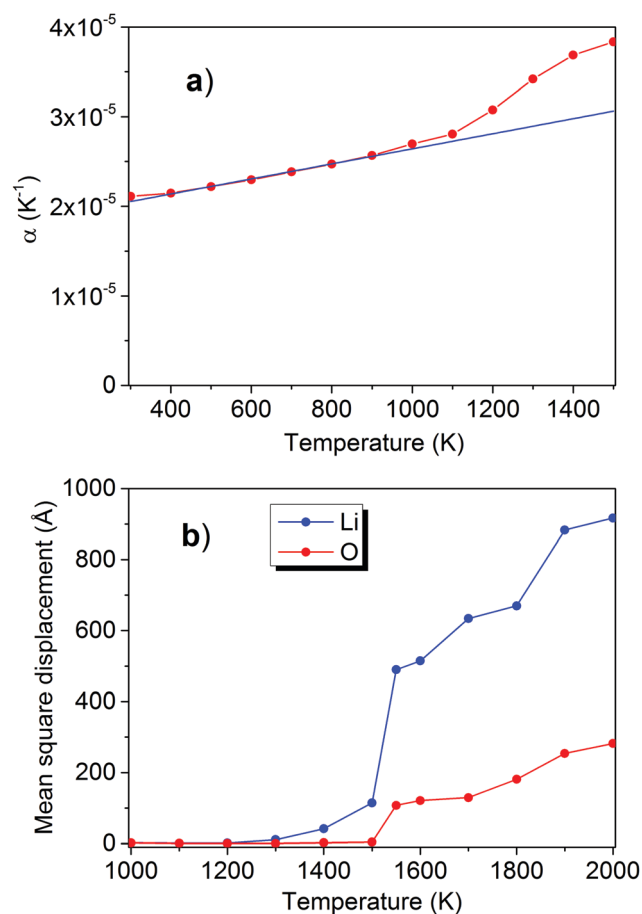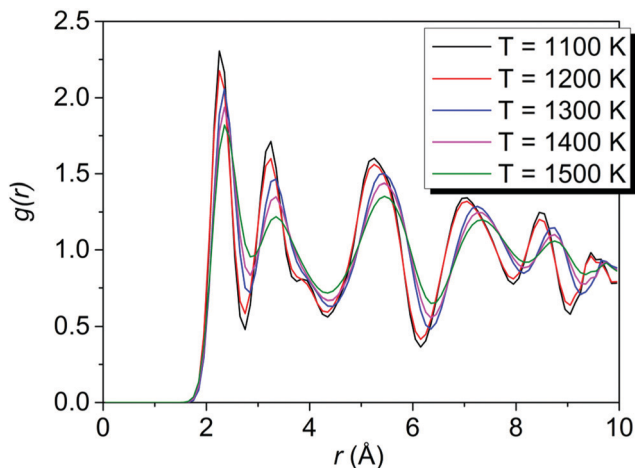
14970 | $Phys. Chem. Chem. Phys.$, 2019, 21, 14964–14972

This journal is © the Owner Societies 2019

Fig. 10 Radial distribution function g(Li–Li), calculated at temperatures between 1100 and 1500 K.

mean square displacement cannot be directly related to the diffusion coefficient in Monte Carlo simulations, it can still be used to estimate atomic mobility.[53,54] We calculated the mean square displacements of the Li and O ions during the accumulation stage of the simulations and Fig. 9b plots these values as a function of temperature (Fig. 9b). Unlike O, Li ions begin to move away from their crystallographic positions at temperatures well below the melting point. It is interesting to note that the superionic transition does not cause substantial changes in the radial distribution function g(Li–Li) (Fig. 10). There is no broadening of the peaks and the function itself resembles closely those of conducting ions in superionics $SrCl_2$ and CaF_2.[55,56]

6. Conclusions

In this work, we had two aims: (i) to investigate the applicability of quantum-corrected Monte Carlo corrections to a real rather than model system and to estimate the importance of these corrections and (ii) to investigate whether the interatomic interaction potential developed in ref. 25 can describe all the most important properties of Li_2O, including the low temperature unit cell size and temperature dependence, solid state diffusion, superionic transition and melting. The use of the quantum-corrected path-integral Monte Carlo method in which each of the atoms is replaced by a ring-like "molecule" consisting of several atoms of the same species increases the applicability of the simulations down to very low temperatures where quantum corrections are important. Several runs with the number l of atoms in a "molecule" increasing from 1 to 8 is sufficient to estimate values of H and a in the limit of infinite l. Values of the unit cell parameter and the enthalpy obtained by this method polynomially (see eqn (5) and (6) and Fig. 3) approach corresponding values at very low temperature, and are in excellent agreement with those obtained using lattice dynamics to calculate the free energy directly in the quasiharmonic approximation. Extrapolations of high-temperature behaviour of $a(T)$ to the low temperatures that use a leading linear term in the temperature,

as carried out in previous studies, do not give the correct low-temperature limit, which is important when comparing theory and experiment.

In the medium temperature range (300–1000 K), we calculated enthalpies of formation of Frenkel and Schottky defects and compared their values with those from direct free energy minimisation in the quasiharmonic approximation. The direct minimisation values fall off more rapidly with temperature than the Monte Carlo results, and this can be substantial even at 500 K. This is associated with the onset of the failure of the quasiharmonic approximation even at relatively modest temperatures and has wider implications for the calculation of defect energies at elevated temperatures in that the temperature variation will be less than quasiharmonic values indicate.

We also investigated the nature of Li diffusion and estimated the migration energy of the Li-vacancy jump. All results are in very good agreement with available experimental data. In particular, the migration energy of the Li-vacancy jump agrees very well with the most recent NMR study.[43] Above 1000 K, the potential[25] is able to describe the superionic transition in the cation subsystem and the melting of the crystal. Temperatures of both transitions were found in good agreement with experiment. The superionic transition manifests itself in our simulations in a rapid rise in the heat capacity which continues until the melting point and two interesting questions remain for future experimental studies: (i) whether above the superionic transition the heat capacity and the linear expansion coefficient rise up to the melting point, as in our simulations, or fall, as with similar fluorites, and (ii) the change in the heat capacity during melting. Further possible work important for fusion applications includes potential based Monte Carlo and *ab initio* investigations of the long-standing problem of tritium behaviour in the Li_2O lattice.[57–59]

Conflicts of interest

There are no conflicts of interest to declare.

Acknowledgements

References

1 J. G. van der Laan, *et al.*, *J. Nucl. Mater.*, 2000, **283–287**, 99.
2 M. J. Sadowski, *Nukleonika*, 2015, **60**, 331.
3 Y. Oishi, *et al.*, *J. Nucl. Mater.*, 1979, **87**, 341.
4 S. Hull, *et al.*, *J. Nucl. Mater.*, 1988, **160**, 125.
5 T. W. D. Farley, *et al.*, *J. Phys.: Condens. Matter*, 1991, **3**, 4761.
6 Y. Y. Liu, *et al.*, *Fusion Technol.*, 1985, **8**, 1970.
7 M. S. Ortman and E. M. Larsen, *J. Am. Ceram. Soc.*, 1983, **66**, 645.
8 T. Matsuo, *et al.*, *J. Chem. Soc., Faraday Trans. 2*, 1983, **79**, 1205.

9 Y. S. Oei and H. Richtering, *Ber. Bunsenges. Phys. Chem.*, 1976, **80**, 1007.

10 A. D. Mulliner, *et al.*, *Phys. Chem. Chem. Phys.*, 2015, **17**, 21470.

11 D. L. Smith, *et al.*, *Fusion Technol.*, 1985, **8**, 10.

12 M. B. Taylor, *et al.*, *Faraday Discuss.*, 1997, **106**, 377.

13 M. B. Taylor, *et al.*, *Phys. Rev. B: Condens. Matter Mater. Phys.*, 1997, **56**, 14380.

14 M. B. Taylor, *et al.*, *Comput. Phys. Commun.*, 1998, **109**, 135.

15 J. D. Gale and A. L. Rohl, *Mol. Simul.*, 2003, **29**, 291.

16 J. D. Gale, *Z. Kristallogr.*, 2005, **220**, 552.

17 D. Frenkel and B. Smit, *Understanding Molecular Simulation*, Academic Press, San Diego, 2nd edn, 2002.

18 N. Metropolis, *et al.*, *J. Chem. Phys.*, 1953, **21**, 1087.

19 R. P. Feynman and A. R. Hibbs, *Quantum mechanics and path integrals*, McGraw-Hill, New York, 1965.

20 M. P. Allen and D. J. Tildesley, *Computer simulation of liquids*, Oxford University Press, 2nd edn, 2017.

21 D. Chandler and P. G. Wolynes, *J. Chem. Phys.*, 1981, **74**, 4078.

22 T. Oda, *et al.*, *J. Nucl. Mater.*, 2007, **367–370**, 263.

23 T. X. T. Sayle, P. E. Ngoepe and D. C. Sayle, *J. Mater. Chem.*, 2010, **20**, 10452.

24 R. Asahi, *et al.*, *Modell. Simul. Mater. Sci. Eng.*, 2014, **22**, 075009.

25 R. M. Fracchia, *et al.*, *J. Phys. Chem. Solids*, 1998, **59**, 435.

26 K. S. Schweizer, *et al.*, *J. Chem. Phys.*, 1981, **75**, 1347.

27 T. H. K. Barron, J. G. Collins and G. K. White, *Adv. Phys.*, 1980, **29**, 609.

28 T. H. K. Barron and G. K. White, *Heat Capacity and Thermal Expansion at Low Temperatures*, Plenum, New York, 1999.

29 H. J. Monkhorst and J. D. Pack, *Phys. Rev. B: Solid State*, 1976, **13**, 5188.

30 R. Juza, W. Uphoff and W. Gieren, *Z. Anorg. Allg. Chem.*, 1957, **292**, 71.

31 R. Dovesi, *et al.*, *Chem. Phys.*, 1991, **156**, 11.

32 J. García Rodeja, M. Meyer and M. Hayoun, *Modell. Simul. Mater. Sci. Eng.*, 2001, **9**, 81.

33 X.-F. Li, *et al.*, *Solid State Commun.*, 2006, **139**, 197.

34 A. V. Chadwick, *et al.*, *Solid State Ionics*, 1988, **28–30**, 185.

35 A. V. Chadwick, *Philos. Mag. A*, 1991, **64**, 983.

36 P. W. M. Jacobs and M. L. Vernon, *J. Chem. Soc., Faraday Trans.*, 1990, **86**, 1233.

37 J. L. Gavartin, *et al.*, *Modell. Simul. Mater. Sci. Eng.*, 1992, **1**, 29.

38 A. De Vita, *et al.*, *Europhys. Lett.*, 1992, **19**, 605.

39 P. Goel, N. Choudhury and S. L. Chaplot, *J. Phys.: Condens. Matter*, 2007, **19**, 386239.

40 J. H. Harding, *Rep. Prog. Phys.*, 1990, **53**, 1403.

41 G. De Lorenzi, G. Jacucci and C. P. Flynn, *Phys. Rev. B: Condens. Matter Mater. Phys.*, 1987, **36**, 9461.

42 M. M. Islam, T. Bredow and C. Minot, *J. Phys. Chem. B*, 2006, **110**, 9413.

43 P. Heitjans and S. J. Indris, *J. Phys.: Condens. Matter*, 2003, **15**, 1257.

44 M. K. Gupta, *et al.*, *Phys. Rev. B: Condens. Matter Mater. Phys.*, 2012, **85**, 184304.

45 T. Tanifuji, K. Shiozawa and S. Nasu, *J. Nucl. Mater.*, 1978, **78**, 422.

46 C. H. Shomate and A. J. Cohen, *J. Am. Chem. Soc.*, 1955, **77**, 285.

47 E. N. Rodigina and K. Z. Gomelskii, *Russ. J. Phys. Chem.*, 1961, **35**, 898.

48 I. Barin and O. Knacke, *Thermochemical Properties of Inorganic Substances*, Springer-Verlag, Berlin, 1973, vol. 416.

49 M. Wilson, S. Jahn and P. A. Madden, *J. Phys.: Condens. Matter*, 2004, **16**, S2795.

50 M. O'Keeffe and B. G. Hyde, *Philos. Mag.*, 1976, **33**, 219.

51 C. E. Derrington, A. Navrotsky and M. O'Keeffe, *Solid State Commun.*, 1976, **18**, 47.

52 R. B. Roberts and G. K. White, *J. Phys. C: Solid State Phys.*, 1986, **19**, 7167.

53 D. Frenkel and A. J. C. Ladd, *J. Chem. Phys.*, 1984, **81**, 3188.

54 H. M. Polatoglou and G. L. Bleris, *Interface Sci.*, 1994, **2**, 31.

55 M. Dixon and M. J. Gillan, *J. Phys. C: Solid State Phys.*, 1980, **13**, 1919.

56 P. J. D. Lindan and M. J. Gillan, *J. Phys.: Condens. Matter*, 1993, **5**, 1019.

57 R. Shah, A. D. Vita and M. C. Payne, *J. Phys.: Condens. Matter*, 1995, **7**, 6981.

58 R. Shah, *et al.*, *Phys. Rev. B: Condens. Matter Mater. Phys.*, 1996, **53**, 8257.

59 T. Oda and S. Tanaka, *J. Nucl. Mater.*, 2011, **417**, 743.

14972 | *Phys. Chem. Chem. Phys.*, 2019, **21**, 14964–14972

This journal is © the Owner Societies 2019